

A novel proxy for tracking the provenance of dust based on paired E₁'-peroxy paramagnetic defect centres in fine-grained quartz

Aditi K. Dave^{1,7*}, Alida Timar-Gabor^{2,3}, Zuzanna Kabacińska², Giancarlo Scardia⁴, Nosir Safaraliev⁵, Saida Nigmatova⁶, Kathryn E. Fitzsimmons^{1,7}

¹Research Group for Terrestrial Palaeoclimates, Max Planck Institute for Chemistry, Hahn-Meitner-Weg 1, 55128 Mainz, Germany

²Faculty of Environmental Sciences and Engineering, Babes Bolyai University, Fantanele 30, Cluj-Napoca, Romania

³Interdisciplinary Research Institute on Bionanoscience, Babes Bolyai University, Treboniu Laurean 42, Cluj-Napoca, Romania

⁴Instituto de Geociências e Ciências Exatas, Universidade Estadual Paulista (UNESP), 13506-900 Rio Claro, SP, Brazil

⁵Tajik National University, 17 Rudaki Avenue, Dushanbe 734025, Tajikistan

⁶Institute of Geological Sciences K. Satpaeva, Ministry for Education and Science of the Republic of Kazakhstan, Almaty, Kazakhstan

⁷Geo- und Umweltforschungszentrum, Department of Geosciences, University of Tuebingen, Schnarrenbergstr. 94-96, 72076 Tuebingen, Germany

*Present address

Corresponding author: Aditi K. Dave (aditikrishna.dave@gmail.com)

Key Points

- New sediment provenance tool exploits E₁' and peroxy paramagnetic defects in quartz
- New proxy successfully differentiates quartz in loess from two different basins in Central Asia
- Potential applications for identifying climate-driven source change through time in loess and other sedimentary sequences

Abstract

Crystal lattice defects in quartz have long been exploited for age determination, yet also show potential for sediment provenance studies. Here we introduce a novel method for tracking aeolian dust provenance by utilising the natural accumulation of E₁' and peroxy defect centres in quartz. Our approach is based on the previously observed premise that E₁' and peroxy centres arise from Frenkel defect pairs, and that their concentration increases with age of the quartz-bearing source rock. We propose that these defect centres can be utilised as a characteristic feature of the source rock and consequently, for fingerprinting sediments derived from it. We successfully apply our new protocol to distinguish fine-grained quartz extracted from loess deposits from two regions in Central Asia which are known to derive from different source

material of differing age. Our method offers strong potential for identifying variability in source, both spatially and through time down sedimentary sequences.

Plain Language Summary

Identifying the origins of dust deposits allows us to reconstruct sediment transport pathways which are essential for understanding past atmospheric circulation patterns. Here we propose to exploit the characteristics of two naturally occurring defect centres in crystalline quartz, the E_1' and peroxy centres, as a means to distinguish sediment deriving from different origins. These centres occur as pairs and are hypothesised to increase with the age of the quartz-bearing rock. By this logic, the E_1' and peroxy centres can be used to determine the lithic origins of sedimentary quartz in a similar way to detrital zircon-based provenance techniques, while analysing a more ubiquitous mineral (quartz). We apply our approach, which uses a simplified protocol for measurement in contrast to earlier studies, to successfully distinguish between loess (wind-blown dust deposits) from two different basins in Central Asia. Our new method holds great potential in its application to loess sequences as well as other sedimentary archives.

Keywords: Provenance, Quartz, Defect centres, Loess, Electron Spin Resonance

1. Introduction

Identifying the original source rocks of sediments is important for understanding sediment cycling. For aeolian sediments, pinpointing provenance has additional advantages of facilitating the reconstruction of transport pathways that relate to atmospheric circulation, and thereby changes in climate dynamics through time. Aeolian loess deposits have long been recognised as valuable archives of past climates in terrestrial environments (Kukla, 1988; Schaetzl et al., 2018). Loess sequences represent long-term accumulation of aeolian dust and thus identifying their provenance provides an important proxy for reconstructing changes in atmospheric circulation through time. A number of established tools are used to identify the source of dust in loess deposits. These include grain-size analysis, in particular grain sorting and end-member modelling, to elucidate transport modes and likely source area types (Vandenberghe, 2013; Li et al., 2018); major and trace elemental composition of bulk dust (Sun et al., 2002; Újvári et al., 2008); radiogenic isotope signatures (Sr and Nd) characteristic of

clay minerals (Chen et al., 2007; Rao et al., 2015; Ben-Israel et al., 2015); and detrital zircon age profiles (Pullen et al., 2011). Whilst these methods are widely used to identify relative changes in dust sources through time, they rely either on materials found in very low concentrations (e.g. detrital zircons) or aggregated bulk measurements from multiple size fractions which are likely to have been transported from both distal and proximal sources (e.g. major and trace elements, radiogenic isotopes). Furthermore, post-depositional weathering can alter *in situ* chemical signatures within loess, rendering certain analytical techniques, if uncorrected, inaccurate for provenance (Yang et al., 2001).

Given the limitations of the above-mentioned provenance techniques, there has been increasing interest in the characteristics of mineral quartz as a tool for linking dust sources and sinks. There are obvious advantages in using quartz as a provenance tool: not only is it ubiquitous, but also highly resistant to weathering and diagenesis (Goldich, 1938). A number of quartz-specific petrographic, isotopic and geochemical provenance methods have been proposed (Bernet & Basset, 2005; Nagashima et al., 2007, 2017; Shimada et al., 2013; Ackerson et al., 2015). Of these, electron spin resonance (ESR) signal of various defect centres in quartz has been increasingly applied to fingerprint sources in sedimentary settings (Nagashima et al., 2007, 2011; Tissoux et al., 2015; Wei et al., 2020).

ESR measures the intensity of paramagnetic species (containing an unpaired electron) in a material. Lattice defects and impurities in quartz give rise to various paramagnetic defect centres. E_1' is one such centre (Weil, 1984), comprising an unpaired electron in an oxygen vacancy ($\equiv Si\cdot$, Fiegl et al., 1974) that are known to arise from diamagnetic oxygen vacancies ($Si=Si$, Jani et al., 1983). The most commonly used ESR based provenance protocol utilises the heat treated- E_1' (hereafter referred to as HT- E_1') intensity of quartz by measuring the intensity of the E_1' centre following gamma (γ) irradiation and thermal treatment (Toyoda & Hattori, 2000; Toyoda et al., 2016). It is based on the premise that γ -irradiation and subsequent heating facilitate conversion of quartz diamagnetic oxygen vacancies into paramagnetic E_1' centres resolvable by ESR and expressed as HT- E_1' . The HT- E_1' intensity has been observed to increase with rock age (Toyoda et al., 1992) and is assumed to reflect the total number of oxygen vacancies, which is characteristic of the rock type and consequently of the source rock from which the quartz is derived (Toyoda & Hattori, 2000; Toyoda et al., 2016). The HT- E_1' intensity is utilised in combination with the crystallinity index of quartz as a common

provenance tool (Nagashima et al, 2007, 2011; Toyoda et al., 2016), since the combination of these is interpreted to reflect the age, formation and crystallisation conditions of quartz in the source rock.

Here we investigate a simplified new provenance method based solely on the analysis of two naturally occurring paramagnetic defect centres in quartz, the E_1' and peroxy centres, using ESR. The formation and characteristics of E_1' and peroxy centres in natural and artificial quartz have long been the subject of empirical study (Weeks, 1956; McMorris, 1970; Stapelbroek et al., 1979; Friebele et al., 1979). Odom and Rink (1989), however, were the first to observe that E_1' and peroxy signals in quartz increase with the age of granitic host rocks, and are positively correlated. Following which, Rink and Odom (1991) proposed that these defect centres arise from Frenkel defect pairs formed by alpha-recoil nuclei, emitted by alpha-emitting elements (U and Th) and accumulated in rocks through time. If this principle holds true for all rock types and the mechanisms for defect formation are understood, then the E_1' and peroxy signals have obvious applications not only as geochronometers (Odom & Rink, 1989) but also for sediment provenance. In this study, we investigate and apply this new method to distinguish quartz in loess sediments from inland Asia. Additionally, we compare the natural E_1' with HT- E_1' characteristics to elucidate differences between our new method and the previous approach (Toyoda and Hattori, 2000).

Inland Asia represents one of the world's major atmospheric dust source, both past and present (Kok et al., 2021), and has been the regional focus for investigations using ESR signals of quartz as a provenance technique (Sun et al., 2007, 2008). The basins to the north, east and west of the Asian high mountains (the Pamirs, Alai-Altai and Tien Shan) lie in topographic rain shadows and represent substantial sinks for glacially- and fluvially-derived sediment from the uplands (Schaetzl et al., 2018; Figure 1). In particular, the loess deposits of arid Central Asia (ACA) and the Chinese Loess Plateau (CLP) reach hundreds of metres in thickness (Liu, 1985; Li et al., 2015) representing long-term substantial accumulation, and by extension, likely distal sources of global aeolian dust. Distinguishing between various potential dust sources in inland Asia is important at multiple scales. At regional levels, identifying changes in source down loess sequences enables reconstruction of variability in dust transport pathways and atmospheric circulation through time. At global scales, it can help identify the relative contributions of different basins to the generic "Asian" mineral dust identified in Greenland

ice cores (Svensson et al., 2000; Bory et al., 2003) and Pacific Ocean marine sediments (Nakai et al., 1993; Letelier et al., 2019).

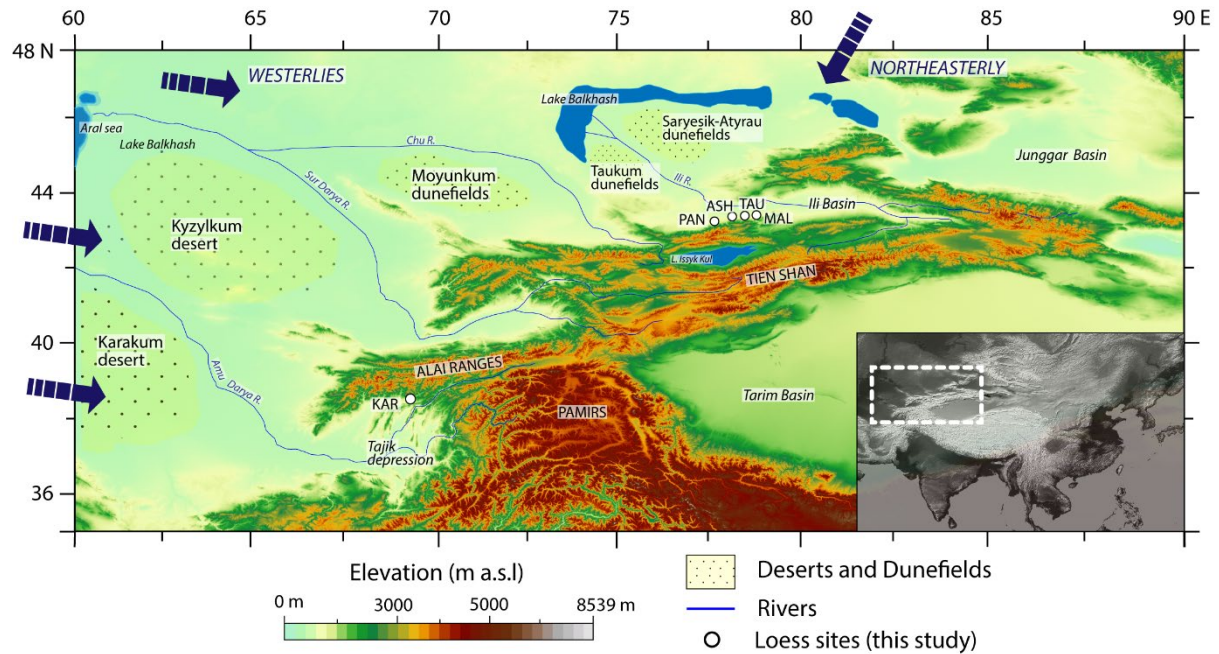


Figure 1. Regional setting and location of the loess sites under study. The elevation map was created using SRTM (Shuttle Radar Topography Mission) data provided by AW3D of the Japan Aerospace Exploration Agency.

In this study, we characterise the natural E_1' and peroxy centre intensities of loess from two basins in ACA, the Ili basin and Tajik depression of southeast (SE) Kazakhstan and Tajikistan respectively (Figure 1). Recent studies based on geochemical fingerprinting and back trajectory analysis indicate that these two loess regions derive sediment from different source areas (Li et al., 2018; Li et al., 2019; Fitzsimmons et al., 2020). The potential significance of the region for global atmospheric dust loads past and present, coupled with the likely discrete sources for

the two basins, make them well suited for targeted spatial and temporal comparison of quartz characteristics for provenance using our new method.

2. Material and Methods

We undertook measurements on fine-grained (4–11 μm) quartz extracted from loess samples collected from five loess sections in Central Asia (Figure 1 and Figure S1). Four of these sections, Panfilov (PAN), Ashubulak (ASH), Taukaraturyuk (TAU) and Malubai (MAL), are located along a c. 200 km east-west transect of the Zailiysky-Alatau range in the Ili basin of SE Kazakhstan. The fifth site, Karamaidan (KAR), is a c. 60 m-thick partial section of a c. 130 m-thick loess-paleosol sequence, located in the foothills of the Gissar mountain range on the northern margins of the Tajik Depression, in southern Tajikistan (Figure 1). We analysed 114 samples; 59 from SE Kazakhstan and 55 from Tajikistan. A detailed account of sampling, site description and age-range, sample preparation, instrumentation and measurement protocols are provided in the Supporting Information (SI).

We performed two sets of experiments on fine-grained quartz:

- (i) To test our new approach, we measured the intensity of E_1' and peroxy centres for all samples. These measurements were conducted on natural quartz samples as is, without any prior treatment and we hereafter refer to these measurements as the natural E_1' and peroxy intensity.
- (ii) To understand differences between our new approach and the previous ESR-based provenance method, we measured the HT- E_1' intensity following published protocols (Toyoda & Hattori, 2000; Nagashima et al., 2007) and compared them to the natural E_1' intensity for all our samples. This involved irradiating all the samples with a γ -dose of 2000 Gy, followed by heating them to 350 °C for 15 minutes to obtain the HT- E_1' intensity. Further, we test our approach and evaluate the need for γ -irradiation and thermal treatment prior to E_1' measurement, by investigating the variation of ESR centres (E_1' , peroxy and Al-hole) with γ -irradiation (varying from 0 to 40000 Gy) and temperature (300, 350 and 400 °C) for two representative samples, one from Kazakhstan (A0016, TAU) and the other

from Tajikistan (A0329, KAR). Detailed descriptions of experimental parameters are given in the SI.

3. Results and Discussion

3.1. Paired E_1' -peroxy centres in quartz: Methodological considerations linking quartz crystal defect dynamics to provenance

Our measurements of the natural E_1' and peroxy intensities of 114 Kazakh and Tajik samples indicate that the natural intensity of E_1' and peroxy centres yield a positive correlation, with a Pearson coefficient of 0.72 (Figure 2a). This supports the hypothesis that these ESR centres indeed arise from Frenkel defect pairs in quartz as per Odom and Rink (1989), and justifies our exploration of both the natural E_1' and peroxy signals for their application as indicators of provenance.

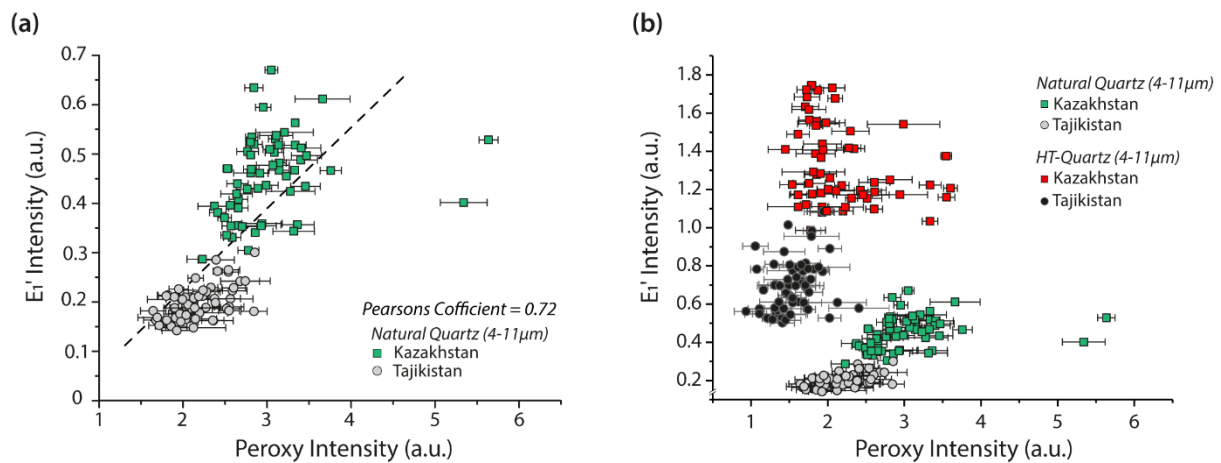


Figure 2. (a) Cross-plot of natural E_1' and peroxy centre intensities of fine-grained quartz from Kazakhstan and Tajikistan based on our new approach; **(b)** Comparison between natural and heat-treated (HT) E_1' and peroxy intensities.

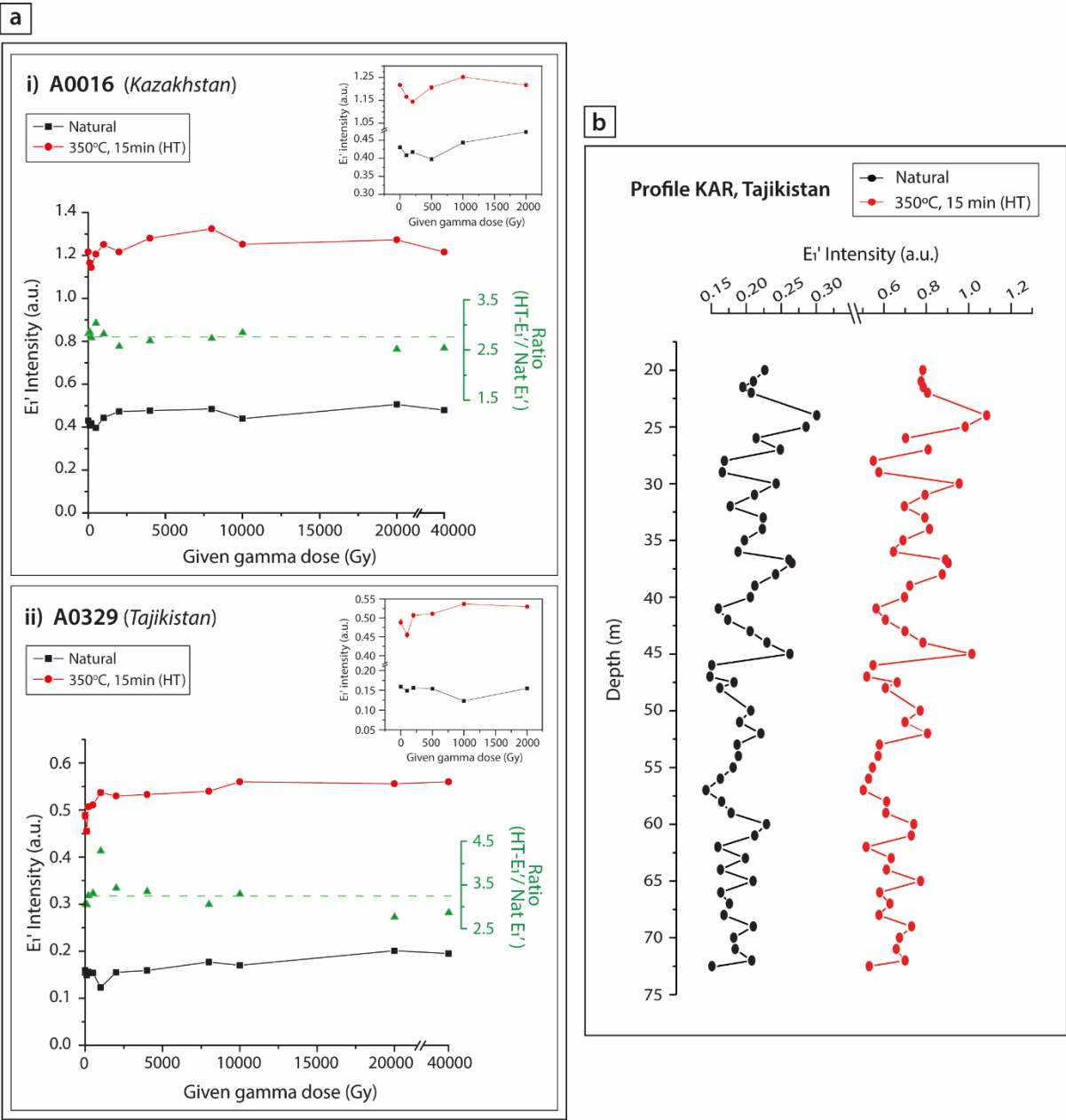
Although intuitive, the measurement of ‘natural’ signals for provenance remains largely unexplored. Our provenance approach, based on natural E_1' and peroxy signals, represents a

simpler protocol than the hitherto established method based on HT-E₁' intensity (Toyoda et al., 2016, and references therein). Figure 2b compares the natural E₁' and HT-E₁' results for all samples. We observe that γ -irradiation and heating simply increases the signal intensity beyond the natural E₁' in all samples. This indicates that the natural E₁' intensity produces the same inherited provenance characteristics as HT-E₁' intensity, and implies that γ -irradiation and heating may not be necessary for our samples.

The proposed mechanism for formation of the HT-E₁' in the established provenance protocols (Toyoda & Ikeya, 1991; Toyoda & Hattori, 2000) suggests that γ -irradiation creates hole-supplying Al-hole centres (which arise from Al impurities in quartz), and post-irradiation heating causes the migration of holes from the Al-hole centres. The released holes recombine with one of the two electrons of the diamagnetic oxygen vacancies, giving rise to an oxygen vacancy with an unpaired electron, i.e. an E₁' centre. Therefore, γ -irradiation and thermal treatment essentially converts all diamagnetic oxygen vacancies - which are characteristic of a given rock - into E₁' centres, known as HT-E₁' centres (Toyoda et al., 2016, and references therein). Meanwhile our results on natural E₁' measurements suggest that sample pre-treatment by γ -irradiation and heating is unnecessary for ESR-based quartz provenance methods. Therefore, we undertook an additional series of irradiation and heating experiments on two representative samples, A0016 (Kazakhstan) and A0329 (Tajikistan), to systematically assess the effects of γ -irradiation and thermal treatment on ESR centres (E₁', peroxy, Al-hole centre), and whether such pre-treatment is necessary for ESR-based provenance studies.

First, we tested the effect of γ -irradiation on the ESR intensity of natural E₁', peroxy and Al-hole centres. We irradiated 11 aliquots of each sample with a γ -dose varying from 0 to 40000 Gy and measured the intensity of each centre. We observe that, overall, the natural E₁' intensity does not change with γ -irradiation (Figure 3a). Our observations corroborate with results obtained from fine-grained quartz from other regions (eastern Europe and North America; Figure S2). Likewise, the natural intensity of the peroxy centre for both samples does not vary with γ -dose (Figure S3). We note that the uncertainty for repeat measurements on the same aliquot for peroxy signal (Figure S3) is 10-20% higher than for the natural E₁', which has an uncertainty of <1%. This is most likely due to the weak peroxy signal observed in our samples.

220 By contrast, the natural Al-hole centre intensity increases exponentially with increasing γ -dose
 221 (Figure S4).



222 **Figure 3.** Variation in natural E_1' and HT- E_1' (350 °C for 15 min) intensity of fine-grained
 223 quartz **(a)** with γ -dose for sample (i) A0016 and (ii) A0329. The inset in each plot shows the
 224 variation over the lower dose range (0-2000 Gy) for the respective sample; **(b)** with depth (or
 225 increasing absorbed dose) at site KAR.
 226

227

Second, we tested the effect of temperature on irradiated quartz E_1' and peroxy centres for the same two representative samples (A0016 and A0329). All γ -irradiated aliquots ($n=11$) of each sample were heated to 300, 350 and 400 °C for 15 min, followed by measurement of the resulting E_1' and peroxy centre intensities. In both samples, E_1' intensity increases with temperature, peaks at 350 °C, and thereafter decreases (Figure S5a, b). The E_1' intensity at any given temperature does not change with increasing γ -dose (Figure S5c, d), which can also be seen in the constant ratio of HT- E_1' to natural E_1' intensity for both samples (Figure 3a). In contrast, the peroxy signal shows minimal change in average intensity with increased temperature (Figure S6). However, the generally weak peroxy signals produce high scatter in the data, rendering assessment of peroxy intensity response to increasing temperature difficult.

Our experiments on fine-grained quartz have two important implications for measuring natural E_1' as a provenance signal. First, E_1' and HT- E_1' intensity remains unchanged with increasing γ -dose, and the ratio between the two signals remains constant (Figure 3a). This suggests that heating increases net E_1' intensity, and irradiation has no effect. This is the case not only for our samples from two regions in Central Asia, but also for detrital quartz from modern river sediments (Wei et al., 2017). We conclude that natural E_1' reflects the quartz characteristics just as well as the HT- E_1' signal and argue that γ -irradiation and heating is not necessary. Second, in both our samples, the intensity of the Al-hole centre increases with increasing γ -dose, in contrast to natural E_1' and HT- E_1' . If we assume the proposed formation mechanism of HT- E_1' centre to be true (Toyoda & Ikeya, 1991; Toyoda & Hattori, 2000), our observations imply that the number of diamagnetic oxygen vacancies in our samples is less than the number of holes released from Al-centres upon heating, even for unirradiated samples. This further sustains our view that the γ -irradiation step is redundant for our samples.

Our work is based on the premise that naturally occurring E_1' and peroxy centres accumulate in rocks over million-year time scales, primarily due to the effect of heavy particle irradiation and thereby show an increase with rock age (Odom and Rink, 1989). Therefore, the use of these defect centres as provenance indicators relies on the fact that their intensity does not change significantly with ionising radiation received during transport and/ or burial as a result of the short time spent by quartz in sedimentary settings as compared to that in the source rock. A recent study by Toyoda and Amimoto (2021) suggests that apart from ionising radiation received in rocks, exposure to radiation during its sedimentary history is also likely to alter the

E_1' signature of quartz. We, therefore provide further evidence that the E_1' signal is independent of ionising radiation received during transport and/ or burial by examining the natural E_1' and HT- E_1' intensity variation with depth down a c. 60 m thick loess section at KAR, Tajikistan. Based on previous (Forster & Heller, 1994) and our own magnetic susceptibility measurements, we correlated the sampled part of the KAR profile to marine oxygen isotope stages (MIS) 19-9 (c. 800–300 ka, Figure S7; Lisiecki & Raymo, 2005). This correlation places the samples from this section beyond the limits of quartz optically stimulated luminescence (OSL) dating. Hence, we estimated the minimum absorbed dose (natural burial dose) received by the uppermost sample to c. 1000 Gy using the post-infrared infrared stimulated luminescence protocol (Table S; Buylaert et al., 2012) on polymineral fine-grains (Figure S8). Assuming a dose rate of 3-4 Gy/ka, which is typical for loess, all samples below the uppermost sample would have received ionising radiation corresponding to an absorbed dose of c. 1000 to 3000 Gy down the profile. The measurement of natural E_1' and HT- E_1' intensity with depth at KAR shows no discerning patterns of incremental increase or decrease (Figure 3b). Whilst, laboratory γ -irradiation experiments on the E_1' signal shows minor variations in the lower dose range (0-2000 Gy; wherein the E_1' intensity first decreases and then increases), unlike that at higher doses (>2000 Gy; Figure 3a). This raises an interesting observation regarding the response of E_1' signal to naturally absorbed doses down KAR, which are also likely to vary between c.1000-3000 Gy down the sequence. In Figure 3a, we observe that E_1' intensity in the lower dose range varies by 5-20% of the natural E_1' values for the representative samples, whereas the variation in E_1' values with depth (and absorbed dose) between loess and soil horizons at KAR ranges by c. 30-50% of the average E_1' values (Figure 3b). Here we note that the average E_1' value is biased by the number of samples taken from the loess versus the soil horizons at KAR, hence the percent variation (if any) in E_1' signature at KAR is likely to be higher than suggested. This implies that the change in E_1' value at KAR is not an artefact of ionising radiation received during burial, but rather represents a change in source (see section 3.2).

3.2 Applications in aeolian environments: Examples from Central Asia

The ultimate aim of sedimentary provenance analysis in aeolian environments is to identify whether parent rocks or sedimentary sources can be linked to the loess or desert deposits in question, and additionally to determine the trajectory of dust transport pathways and by extension, the most likely climate circulation patterns prevailing at the time of transport and deposition. Our study provides a critical step towards achieving the aim of identifying provenance within sediments by establishing a simplified protocol exploiting characteristic signatures based on defect centres in quartz.

Our suite of 114 samples forms two distinct spectral clusters depending on geographic region (Figure 2a). Of the two natural ESR signals measured, the natural E_1' intensity yields the greatest difference between the two regions (Figure 2a). The more diffused peroxy signatures are a result of inherently weak peroxy signal in our samples, and may also reflect the hypothesis that ‘peroxy’ signals, as measured, represent the overlap of a peroxy radical ($\equiv Si-O-O\cdot$, POR) and non-bridging oxygen hole centre ($\equiv Si-O\cdot$, NBOHC) (based on observations by Salh, 2011; Skuja et al., 2020; Figure S9). Nevertheless, the peroxy signals from the two regions are statistically distinguishable, and along with the natural E_1' intensity, can be used as provenance indicators.

We observe higher natural E_1' and peroxy signals in the Kazakh loess than the Tajik samples. Since the E_1' and peroxy centres are known to accumulate with time (Odom and Rink, 1989), this suggests that the Kazakh quartz is sourced from older rocks than the Tajik quartz. The suggestion that the Kazakh source rock is older is consistent with the rocks of the central Tien Shan, which are of Palaeozoic age or older (Tursungaziev & Petrov, 2008), and represent the likely source material to the Kazakh loess piedmont (Li et al., 2018; Fitzsimmons et al., 2020). These are older than the predominantly Mesozoic and younger rocks of the Gissar Mountains and northwestern Pamirs (Vlasov et al., 1991), which provide the most likely source rocks for the Tajik loess (Li et al., 2019). The formation of two separate clusters for two independently sourced regions of different source rock age provides support for our proposed approach as a provenance tool.

In addition to differentiating likely source regions for different loess sites, we ultimately aim to identify potential changes in source through time down long sedimentary (including loess) sequences such as those found in inland Asia. Figure 4a shows down-profile variations in

natural E_1' intensity of loessic quartz at KAR in Tajikistan, a site which preserves multiple primary loess and buried soil (paleosol) horizons (refer SI for details). We observe a marked difference in the natural E_1' and peroxy signature in loess versus paleosol horizons (Figure 4b). Recent work using trace element concentrations of loess in Tajikistan, combined with meteorological reanalysis, suggests that provenance is site-dependent and likely to be dominated by proximal montane sites (Li et al., 2016), with some contribution from distal sources such as the Karakum desert (Li et al., 2019). The relative contributions of distal and proximal sources to loess deposits in Tajikistan may have changed over glacial-interglacial timescales as a result of changes in the dynamics and intensity of atmospheric circulation. We suggest that our observed changes in paired E_1' -peroxy characteristics represent variability in the dominant source signature of quartz between the primary (glacial) loess and paleosol (interglacial) horizons. At this stage, without more targeted investigations of potential source rocks, we cannot identify whether the change in the dominant source signature through time at KAR is a result of proximal and/or distal transport of dust. Nevertheless, our observations hold promise for more focused investigations of source signature based on our provenance method.

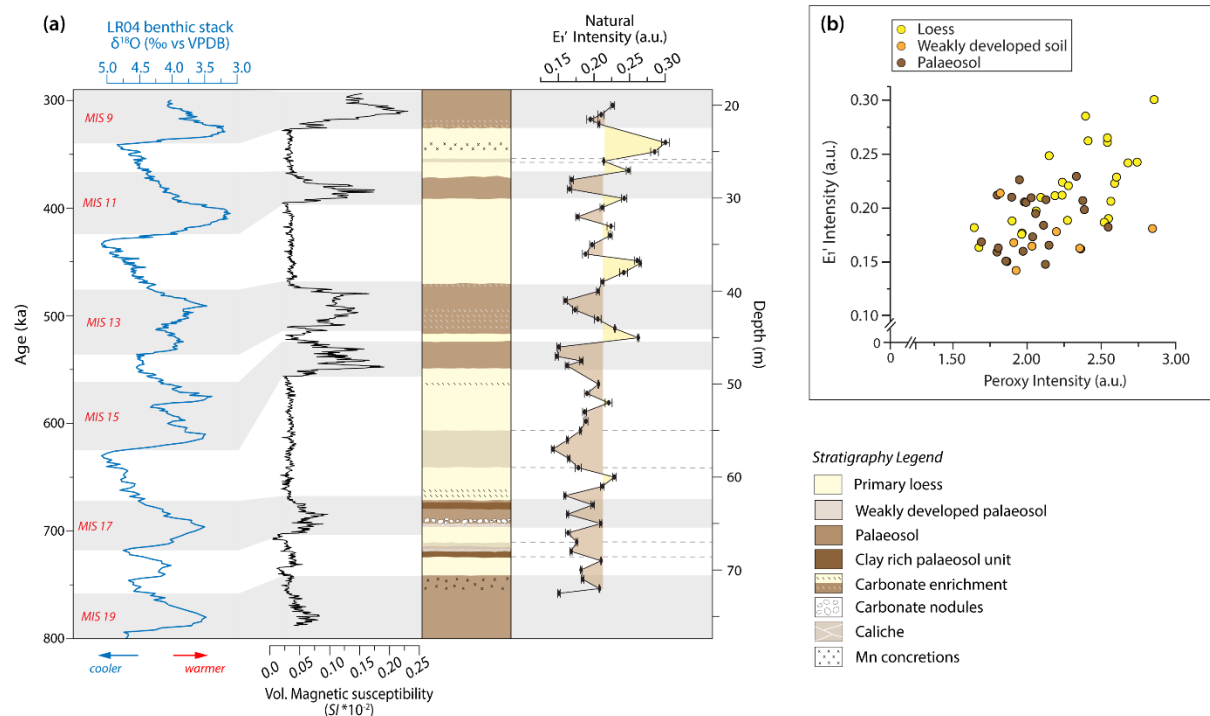


Figure 4. (a) Down-profile variability in E_1' intensity of fine-grained quartz at KAR, Tajikistan. The magnetic susceptibility data was measured in the field (refer SI) while LR04

benthic $\delta^{18}\text{O}$ data was obtained from Lisiecki and Raymo (2005); **(b)** Natural E_1' and peroxy variation in samples from various stratigraphic sections (identified here as loess, palaeosol, and weakly developed palaeosols) at KAR based on field stratigraphic description and magnetic susceptibility data.

4. Conclusion

We propose a new method for determining the provenance of sedimentary quartz based on the natural accumulation of E_1' and peroxy centres. We confirm, based on empirical measurements of 114 fine-grained loessic quartz samples, that firstly, the natural E_1' and peroxy signals are positively correlated and are likely to arise from Frenkel defect pairs. Secondly, the increase in intensity of these centres with age of the source rock can be seen in the higher values obtained from the Kazakh samples, which are derived from older rocks than the Tajik loess. Therefore, quartz from the Ili basin of SE Kazakhstan yields signals distinct from quartz in the Tajik basin in Tajikistan, indicating a difference in provenance consistent with previously published studies. Furthermore, down-profile measurements at the KAR site in Tajikistan indicates a shift in source between primary loess and paleosol horizons, most likely in response to changes in atmospheric circulation associated with climatic oscillations. Thus, our observations suggest this to be a robust new technique for sediment provenance, that can be applicable to a range of settings, exploiting the characteristics of one of the most ubiquitous minerals found in nature: quartz.

Acknowledgements

AK Dave would like to thank the Luminescence Laboratory at the Max Planck Institute for Evolutionary Anthropology, Leipzig, Germany for access to the HF etching laboratory. We also thank the following colleagues for their assistance during fieldwork in Tajikistan: S Yusupov, A Safarov, RS Pavlatov and ZN Nadjmudinov (Tajik National University); C Prud'homme, A Engström Johansson, L Marquer, Z Perić, S de Graaf, M Notwatzki and K Reetz (Max Planck Institute for Chemistry). This study was funded by an independent Max Planck Research Group awarded by the Max Planck Society to K.E. Fitzsimmons. A Timar-Gabor and Z Kabacińska received funding from the European Research Council (ERC) under

the European Union's Horizon 2020 research and innovation programme ERC-2015-STG (grant agreement No [678106]).

References for main text

Ackerson, M. R., Tailby, N. D., & Watson, E. B. (2015). Trace elements in quartz shed light on sediment provenance. *Geochemistry, Geophysics, Geosystems*, 16(6), 1894–1904. <https://doi.org/10.1002/2015GC005896>

Ben-Israel, M., Enzel, Y., Amit, R., & Erel, Y. (2015). Provenance of the Various Grain-Size Fractions in the Negev Loess and Potential changes in Major dust Sources to the Eastern Mediterranean. *Quaternary Research*, 83(1), 105–115. doi:10.1016/j.yqres.2014.08.001

Bernet, M., & Bassett, K. (2005). Provenance analysis by single-quartz-grain SEM-CL/optical microscopy. *Journal of Sedimentary Research*, 75(3), 492–500. <https://doi.org/10.2110/jsr.2005.038>

Bory, A. J.-M., Biscaye, P. E., & Grousset, F. E. (2003). Two distinct seasonal Asian source regions for mineral dust deposited in Greenland (NorthGRIP). *Geophysical Research Letters*, 30(4). <https://doi.org/10.1029/2002GL016446>

Buylaert, J.-P., Jain, M., Murray, A. S., Thomsen, K. J., Thiel, C., & Sohbati, R. (2012). A robust feldspar luminescence dating method for Middle and Late Pleistocene sediments. *Boreas*, 41(3), 435–451. <https://doi.org/10.1111/j.1502-3885.2012.00248.x>

Chen, J., Li, G., Yang, J., Rao, W., Lu, H., Balsam, W., Sun, Y., & Ji, J. (2007). Nd and Sr isotopic characteristics of Chinese deserts: Implications for the provenances of Asian dust. *Geochimica et Cosmochimica Acta*, 71(15), 3904–3914. <https://doi.org/10.1016/j.gca.2007.04.033>

Feigl, F. J., Fowler, W. B., & Yip, K. L. (1974). Oxygen vacancy model for the E1' center in SiO₂. *Solid State Communications*, 14(3), 225–229. [https://doi.org/10.1016/0038-1098\(74\)90840-0](https://doi.org/10.1016/0038-1098(74)90840-0)

Fitzsimmons, K. E., Nowatzki, M., Dave, A. K., & Harder, H. (2020). Intersections between wind regimes, topography and sediment supply: Perspectives from aeolian landforms in Central Asia. *Palaeogeography, Palaeoclimatology, Palaeoecology*, 540, 109531. <https://doi.org/10.1016/j.palaeo.2019.109531>

Forster, Th., & Heller, F. (1994). Loess deposits from the Tajik depression (Central Asia): Magnetic properties and paleoclimate. *Earth and Planetary Science Letters*, 128(3–4), 501–512. [https://doi.org/10.1016/0012-821X\(94\)90166-X](https://doi.org/10.1016/0012-821X(94)90166-X)

Friebele, E. J., Griscom, D. L., Stapelbroek, M., & Weeks, R. A. (1979). Fundamental defect centers in glass: The peroxy radical in irradiated, high-purity, fused silica. *Physical Review Letters*, 42(20), 1346–1349.

Goldich, S. S. (1938). A Study in Rock-Weathering. *The Journal of Geology*, 46(1), 17–58. <https://doi.org/10.1086/624619>

406 Ikeya, M. (1993). New Applications of Electron Spin Resonance: Dating, Dosimetry and
407 Microscopy. World Scientific. <https://doi.org/10.1142/1854>

408 Isozaki, Y., Tada, R., Sun, Y., Zheng, H., Toyoda, S., Sugiura, N., Karasuda, A., & Hasegawa,
409 H. (2020). Origin of aeolian dust emitted from the Tarim Basin based on the ESR signal
410 intensity and crystallinity index of quartz: The recycling system of fine detrital material within
411 the basin. *Geological Magazine*, 157(5), 707–718. Cambridge Core.
412 <https://doi.org/10.1017/S0016756820000242>

413 Jani, M.G., Bossoli, R.B., Halliburton, L.E. (1983). Further characterization of the E1' center
414 in crystalline SiO₂. *Physical Review B* 27, 2285–2293.
415 <https://doi.org/10.1103/PhysRevB.27.2285>

416 Kok, J. F., Adebisi, A. A., Albani, S., Balkanski, Y., Checa-Garcia, R., Chin, M., Colarco, P.
417 R., Hamilton, D. S., Huang, Y., Ito, A., Klose, M., Li, L., Mahowald, N. M., Miller, R. L.,
418 Obiso, V., Pérez García-Pando, C., Rocha-Lima, A., & Wan, J. S. (2021). Contribution of the
419 world's main dust source regions to the global cycle of desert dust. *Atmospheric Chemistry*
420 *and Physics Discussions*, 2021, 1–34. <https://doi.org/10.5194/acp-2021-4>

421 Kukla, G., Heller, F., Ming, L. X., Chun, X. T., Sheng, L. T., & Sheng, A. Z. (1988).
422 Pleistocene climates in China dated by magnetic susceptibility. *Geology*, 16(9), 811–814.
423 [https://doi.org/10.1130/0091-7613\(1988\)016<0811:PCICDB>2.3.CO;2](https://doi.org/10.1130/0091-7613(1988)016<0811:PCICDB>2.3.CO;2)

424 Letelier, R. M., Björkman, K. M., Church, M. J., Hamilton, D. S., Mahowald, N. M., Scanza,
425 R. A., Schneider, N., White, A. E., & Karl, D. M. (2019). Climate-driven oscillation of
426 phosphorus and iron limitation in the North Pacific Subtropical Gyre. *Proceedings of the*
427 *National Academy of Sciences*, 116(26), 12720–12728.
428 <https://doi.org/10.1073/pnas.1900789116>

429 Li, Y., Song, Y., Yan, L., Chen, T., & An, Z. (2015). Timing and Spatial Distribution of Loess
430 in Xinjiang, NW China. *PLOS ONE*, 10(5), e0125492.
431 <https://doi.org/10.1371/journal.pone.0125492>

432 Li, Y., Song, Y., Chen, X., Li, J., Mamadjanov, Y., & Aminov, J. (2016). Geochemical
433 composition of Tajikistan loess and its provenance implications. *Palaeogeography,*
434 *Palaeoclimatology,* *Palaeoecology*, 446, 186–194.
435 <https://doi.org/10.1016/j.palaeo.2016.01.025>

436 Li, Y., Song, Y., Fitzsimmons, K. E., Chen, X., Wang, Q., Sun, H., & Zhang, Z. (2018). New
437 evidence for the provenance and formation of loess deposits in the Ili River Basin, Arid Central
438 Asia. *Aeolian Research*, 35, 1–8. <https://doi.org/10.1016/j.aeolia.2018.08.002>

439 Li, Y., Song, Y., Kaskaoutis, D. G., Chen, X., Mamadjanov, Y., & Tan, L. (2019). Atmospheric
440 dust dynamics in southern Central Asia: Implications for buildup of Tajikistan loess sediments.
441 *Atmospheric Research*, 229, 74–85. <https://doi.org/10.1016/j.atmosres.2019.06.013>

442 Lisiecki, L. E., & Raymo, M. E. (2005). A Pliocene-Pleistocene stack of 57 globally distributed
443 benthic $\delta^{18}\text{O}$ records. *Paleoceanography*, 20(1). <https://doi.org/10.1029/2004PA001071>

444 Liu, T. S. (1985). *Loess and Environment*. China Ocean Press (Beijing).

445 McMorris, D. W. (1970). ESR Detection of Fossil Alpha Damage in Quartz. *Nature*, 226(5241),
446 146–148. <https://doi.org/10.1038/226146b0>

447 Nagashima, K., Tada, R., Tani, A., Toyoda, S., Sun, Y., & Isozaki, Y. (2007). Contribution of
 448 aeolian dust in Japan Sea sediments estimated from ESR signal intensity and crystallinity of
 449 quartz. *Geochemistry, Geophysics, Geosystems*, 8(2). <https://doi.org/10.1029/2006GC001364>
 450 Nagashima, K., Tada, R., Tani, A., Sun, Y., Isozaki, Y., Toyoda, S., & Hasegawa, H. (2011).
 451 Millennial-scale oscillations of the westerly jet path during the last glacial period. *Journal of*
 452 *Asian Earth Sciences*, 40(6), 1214–1220. <https://doi.org/10.1016/j.jseas.2010.08.010>
 453 Nagashima, K., Tada, R., & Toyoda, S. (2013). Westerly jet-East Asian summer monsoon
 454 connection during the Holocene. *Geochemistry, Geophysics, Geosystems*, 14(12), 5041–5053.
 455 Scopus. <https://doi.org/10.1002/2013GC004931>
 456 Nagashima, K., Nishido, H., Kayama, M., Kurosaki, Y., Ohgo, S., & Hasegawa, H. (2017).
 457 Composition of Asian dust from cathodoluminescence spectral analysis of single quartz grains.
 458 *Geology*, 45(10), 879–882. <https://doi.org/10.1130/G39237.1>
 459 Nakai, S., Halliday, A. N., & Rea, D. K. (1993). Provenance of dust in the Pacific Ocean. *Earth*
 460 *and Planetary Science Letters*, 119(1), 143–157. [https://doi.org/10.1016/0012-](https://doi.org/10.1016/0012-821X(93)90012-X)
 461 [821X\(93\)90012-X](https://doi.org/10.1016/0012-821X(93)90012-X)
 462 Odom, A. L., & Rink, W. J. (1989). Natural accumulation of Schottky-Frenkel defects:
 463 Implications for a quartz geochronometer. *Geology*, 17(1), 55–58.
 464 [https://doi.org/10.1130/0091-7613\(1988\)017<0055:NAOSFD>2.3.CO;2](https://doi.org/10.1130/0091-7613(1988)017<0055:NAOSFD>2.3.CO;2)
 465 Pullen, A., Kapp, P., McCallister, A. T., Chang, H., Gehrels, G. E., Garzione, C. N.,
 466 Heermance, R. V., & Ding, L. (2011). Qaidam Basin and northern Tibetan Plateau as dust
 467 sources for the Chinese Loess Plateau and paleoclimatic implications. *Geology*, 39(11), 1031–
 468 1034. <https://doi.org/10.1130/G32296.1>
 469 Rao, W., Tan, H., Chen, J., Ji, J., Chen, Y., Pan, Y., & Zhang, W. (2015). Nd–Sr isotope
 470 geochemistry of fine-grained sands in the basin-type deserts, West China: Implications for the
 471 source mechanism and atmospheric transport. *Geomorphology*, 246, 458–471.
 472 <https://doi.org/10.1016/j.geomorph.2015.06.043>
 473 Rink, W. J., & Odom, A. L. (1991). Natural alpha recoil particle radiation and ionizing
 474 radiation sensitivities in quartz detected with EPR: Implications for geochronometry.
 475 *International Journal of Radiation Applications and Instrumentation. Part D. Nuclear Tracks*
 476 *and Radiation Measurements*, 18(1), 163–173. [https://doi.org/10.1016/1359-0189\(91\)90108-T](https://doi.org/10.1016/1359-0189(91)90108-T)
 477 Salh, R. (2011). Defect Related Luminescence in Silicon Dioxide Network: A Review. In S.
 478 Basu (Ed.), *Crystalline Silicon—Properties and Uses*. InTech. <https://doi.org/10.5772/22607>
 479 Schaetzl, R. J., Bettis, E. A., Crouvi, O., Fitzsimmons, K. E., Grimley, D. A., Hambach, U.,
 480 Lehmkuhl, F., Marković, S. B., Mason, J. A., Owczarek, P., Roberts, H. M., Rousseau, D.-D.,
 481 Stevens, T., Vandenberghe, J., Zárate, M., Veres, D., Yang, S., Zech, M., Conroy, J. L., ...
 482 Zech, R. (2018). Approaches and challenges to the study of loess—Introduction to the
 483 LoessFest Special Issue. *Quaternary Research*, 89(3), 563–618. doi:10.1017/qua.2018.15
 484 Shimada, A., Takada, M., & Toyoda, S. (2013). Characteristics of ESR signals and TLCLs of
 485 quartz included in various source rocks and sediments in Japan: A clue to sediment provenance.
 486 *Geochronometria*, 40(4), 334–340. <https://doi.org/10.2478/s13386-013-0111-z>

487 Skuja, L., Ollier, N., & Kajihara, K. (2020). Luminescence of non-bridging oxygen hole centers
 488 as a marker of particle irradiation of α -quartz. *Radiation Measurements*, 135, 106373.
 489 <https://doi.org/10.1016/j.radmeas.2020.106373>

490 Stapelbroek, M., Griscom, D. L., Friebele, E. J., & Sigel, G. H. (1979). Oxygen-associated
 491 trapped-hole centers in high-purity fused silicas. *Electronic Properties and Structure of*
 492 *Amorphous Solids*, 32(1), 313–326. [https://doi.org/10.1016/0022-3093\(79\)90079-6](https://doi.org/10.1016/0022-3093(79)90079-6)

493 Sun, J. (2002). Provenance of loess material and formation of loess deposits on the Chinese
 494 Loess Plateau. *Earth and Planetary Science Letters*, 203(3), 845–859.
 495 [https://doi.org/10.1016/S0012-821X\(02\)00921-4](https://doi.org/10.1016/S0012-821X(02)00921-4)

496 Sun, Y., Tada, R., Chen, J., Chen, H., Toyoda, S., Tani, A., Isozaki, Y., Nagashima, K.,
 497 Hasegawa, H., & Ji, J. (2007). Distinguishing the sources of Asian dust based on electron spin
 498 resonance signal intensity and crystallinity of quartz. *Atmospheric Environment*, 41(38), 8537–
 499 8548. <https://doi.org/10.1016/j.atmosenv.2007.07.014>

500 Sun, Y., Tada, R., Chen, J., Liu, Q., Toyoda, S., Tani, A., Ji, J., & Isozaki, Y. (2008). Tracing
 501 the provenance of fine-grained dust deposited on the central Chinese Loess Plateau.
 502 *Geophysical Research Letters*, 35(1), L01804. <https://doi.org/10.1029/2007GL031672>

503 Sun, Y., Chen, H., Tada, R., Weiss, D., Lin, M., Toyoda, S., Yan, Y., & Isozaki, Y. (2013).
 504 ESR signal intensity and crystallinity of quartz from Gobi and sandy deserts in East Asia and
 505 implication for tracing Asian dust provenance. *Geochemistry, Geophysics, Geosystems*, 14(8),
 506 2615–2627. <https://doi.org/10.1002/ggge.20162>

507 Svensson, A., Biscaye, P. E., & Grousset, F. E. (2000). Characterization of late glacial
 508 continental dust in the Greenland Ice Core Project ice core. *Journal of Geophysical Research:*
 509 *Atmospheres*, 105(D4), 4637–4656. <https://doi.org/10.1029/1999JD901093>

510 Tissoux, H., Voinchet, P., Lacquement, F., & Despriée, J. (2015). ESR as a method for the
 511 characterization of alluvial sediments. *Radiation Measurements*, 81, 2–8.
 512 <https://doi.org/10.1016/j.radmeas.2015.05.010>

513 Toyoda, S., & Ikeya, M. (1991). Thermal stabilities of paramagnetic defect and impurity
 514 centers in quartz: Basis for ESR dating of thermal history. *Geochemical Journal*, 25(6), 437–
 515 445. <https://doi.org/10.2343/geochemj.25.437>

516 Toyoda, S., Ikeya, M., Morikawa, J., & Nagatomo, T. (1992). Enhancement of oxygen
 517 vacancies in quartz by natural external β and γ ray dose: A possible ESR Geochronometer of
 518 Ma-Ga range. *Geochemical Journal*, 26(3), 111–115. <https://doi.org/10.2343/geochemj.26.111>

519 Toyoda, S., & Hattori, W. (2000). Formation and decay of the E1' center and of its precursor.
 520 *Applied Radiation and Isotopes*, 52(5), 1351–1356. [https://doi.org/10.1016/S0969-8043\(00\)00094-4](https://doi.org/10.1016/S0969-8043(00)00094-4)

522 Toyoda, S., Rink, W. J., Yonezawa, C., Matsue, H., & Kagami, T. (2001). In situ production
 523 of alpha particles and alpha recoil particles in quartz applied to ESR studies of oxygen
 524 vacancies. *TL/ESR Special*, 20(5), 1057–1061. [https://doi.org/10.1016/S0277-3791\(00\)00018-4](https://doi.org/10.1016/S0277-3791(00)00018-4)

526 Toyoda, S., Nagashima, K., & Yamamoto, Y. (2016). ESR signals in quartz: Applications to
 527 provenance research – A review. *Quaternary International*, 397, 258–266.
 528 <https://doi.org/10.1016/j.quaint.2015.05.048>

529 Toyoda S, Amimoto M.(2021). Dose Response of the E1' Centre in Quartz. *Geochronometria*.
530 48(1): 191-196. <https://doi.org/10.2478/geochr-2020-0037>

531 Tursungaziev, B. T., & Petrov, O. B. (Eds.), (2008). Geological Map of the Kyrgyz Republic,
532 1:500,000. Bishkek.

533 Újvári, G., Varga, A., & Balogh-Brunstad, Z. (2008). Origin, weathering, and geochemical
534 composition of loess in southwestern Hungary. *Quaternary Research*, 69(3), 421–437.
535 <https://doi.org/10.1016/j.yqres.2008.02.001>

536 Usami, T., Toyoda, S., Bahadur, H., Srivastava, A. K., & Nishido, H. (2009). Characterization
537 of the E1' center in quartz: Role of aluminum hole centers and oxygen vacancies. *Physica B:
538 Condensed Matter*, 404(20), 3819–3823. <https://doi.org/10.1016/j.physb.2009.07.075>

539 Vandenberghe, J. (2013). Grain size of fine-grained windblown sediment: A powerful proxy
540 for process identification. *Earth-Science Reviews*, 121, 18–30.
541 <https://doi.org/10.1016/j.earscirev.2013.03.001>

542 Vlasov, N., Yu, G., Dyakov, A., and Cherev, E.S. (1991). Geological Map of the Tajik SSR
543 and Adjacent Territories: Saint Petersburg, Russia, Vsesojuznoi Geologic Institute of
544 Leningrad, scale 1:500,000.

545 Weeks, R. A. (1956). Paramagnetic Resonance of Lattice Defects in Irradiated Quartz. *Journal
546 of Applied Physics*, 27(11), 1376–1381. <https://doi.org/10.1063/1.1722267>

547 Wei, C., Li, C., Liu, C., Li, W., Zhang, Z., Zhang, H., Zhao, J., & Zhang, L. (2017). Nature
548 ESR signals of quartz E' center shed new light on river sediments provenance: A case study in
549 southeast margin of the Tibet Plateau. *Third Pole: The Last 20,000 Years - Part III*, 454, 38–
550 44. <https://doi.org/10.1016/j.quaint.2017.08.044>

551 Wei, C., Yin, G., Li, Y., Liu, C., Li, W., Guo, R. (2020). Quartz electron spin resonance signal
552 intensity of Al and Ti–Li centers as a provenance indicator: An example from the Yangtze
553 River Basin. *Quaternary International* 562, 76-84.
554 <https://doi.org/10.1016/j.quaint.2020.06.023>.

555 Weil, J. A. (1984). A review of electron spin spectroscopy and its application to the study of
556 paramagnetic defects in crystalline quartz. *Physics and Chemistry of Minerals*, 10(4), 149–165.
557 <https://doi.org/10.1007/BF00311472>

558 Weltje, G. J., & von Eynatten, H. (2004). Quantitative provenance analysis of sediments:
559 Review and outlook. *Quantitative Provenance Analysis of Sediments*, 171(1), 1–11.
560 <https://doi.org/10.1016/j.sedgeo.2004.05.007>

561 Yang, J.-D., Chen, J., Tao, X.-C., Li, C.-L., Ji, J.-F., & Chen, Y. (2001). Sr isotope ratios of
562 acid-leached loess residues from Luochuan, China: A tracer of continental weathering intensity
563 over the past 2.5 Ma. *Geochemical Journal*, 35(6), 403–412.